Silicon photonics ionic sensor enabled by hybrid integrated 2D plasmonic MoO_3

Guanghui Ren, Baoyue Zhang, Markus Knoerzer, Arnan Mitchell, Jianzhen Ou
Electronics and Telecommunications Engineering, School of Engineering,
RMIT University P.O. Box 2462, Melbourne VIC 3001, Australia
e-mail: Guanghui.ren@rmit.edu.au

ABSTRACT

Silicon photonics has demonstrated great potential in ultra-sensitive biochemical sensing. However, it is challenging for such sensors to detect small ions which are also of great importance in many biochemical processes. Here, we introduce a silicon photonic ion sensor enabled by an ionic dopant-driven plasmonic material. The sensor consists of a micro-ring resonator (MRR) coupled with a two-dimensional (2D) re-stacked layer of near-infrared plasmonic molybdenum oxide. When the 2D plasmonic layer interacts with ions from the environment, a strong change in the refractive index results in a shift in the MRR resonance wavelength and simultaneously the alteration of plasmonic absorption leads to the modulation of MRR transmission power, hence generating dual sensing outputs which is unique to other optical ion sensors. We demonstrate proof-of-concept via a pH sensing model, showing a up to 7 orders improvement on sensitivity per unit area across the range from 1 to 13 compared to those of other optical pH sensors. Our platform offers the unique potential for ultra-sensitive and robust measurement of changes in ionic environment, generating new modalities for on-chip chemical sensors in the micro/nano-scale.

Keywords: integrated optics, silicon photonics, two-dimensional materials, doped semiconductor, ion sensor

1. INTRODUCTION

Silicon photonics has grown into a mature platform that is compatible with complementary metal-oxide–semiconductor (CMOS) technology, offering both wide bandwidth and low propagation loss overcoming the electronic bottleneck currently faced by microelectronics[1-3]. Silicon photonics has also emerged as an effective platform for biochemical sensing based on the perturbation of the evanescent field induced by the optical guided mode[4-7], through either the direct interferometric or resonant sensing of the ambient refractive index. These sensors are normally enabled by the specific interaction of two complementary molecules *via* surface functionalization. Typical examples include the functionalization with selective molecules such as DNA in the silicon photonic sensor for detecting complementary DNA/RNA strain[8, 9]. However, ionic species, which are also vital chemical components in many biochemical processes and metabolic activities of microorganisms, cannot be easily detected with current silicon photonic biosensors as the direct binding of ions onto the surface functional groups does not produce a measurable response of the ambient refractive index[9, 10].

In this regard, the realization of a sensing platform with additional measurable parameters beyond the analyte-induced ambient refractive index change should be of critical relevance for widening the application of silicon photonic based biochemical sensors. Recently, the emerging integration of two dimensional (2D) layered materials onto the silicon photonics platform provides a viable solution to obtain enhanced electronic and optical properties, mechanically flexibility, low fabrication and integration complexity, robustness, all while maintaining compatibility with CMOS technology[11-13].

In this contribution, 2D H^+ doped molybdenum oxides with NIR plasmon resonance is integrated on a silicon based micro-ring resonator to establish the label-free chemical sensing platform. The pH sensing model is used as the representative to evaluate the performance of this novel chemical sensing platform. In contrast, the unique H^+ dopants in the 2D MoO_3 host are hypothesized to be sensitive to the ambient change of ionic species concentration when the pH value is change from very acidic (pH=1) to very alkaline (pH =13) or *vice versa*. As a result, the H^+ dopant driven plasmonics is correspondingly altered and the optical absorption due to the excitation of hybrid plasmonic-optical modes in the silicon micro-ring resonator. Simultaneously, the refractive index of the 2D material also changed due to the variation of H^+ concentration, which leads to the shift of the resonant wavelength of the micro-ring resonator.

2. Design and Fabrication

To realize the 2D H^+ doped MoO_3 – silicon photonic based chemical sensing platform, a relatively high-performance micro-ring resonator (MRR) is firstly fabricated. The MRR is composed of a ring and two bus waveguides (Figure 1a). Grating couplers are used as the interface between the single mode optical fiber and the integrated Si photonic chip. As seen from the SEM image of the bare device (upper image of Figure 1b), the waveguides have width and height of 450 and 220 nm, respectively. The radius of the ring is 10 μm and the

separation distance between the ring and bus waveguide is 150 nm. After fabrication and initial characterization, 2D H^+ doped MoO_3 is deposited onto the micro-ring resonator using PTFE as a binding agent to enhance the adhesion between 2D $H_{0.3}MoO_3$ and the Si waveguide. Most of the surface area of the MRR are covered with 2D $H_{0.3}MoO_3$ nanoflakes with the relatively homogeneous thickness distribution in the region of 150 - 250 nm as evidenced by the SEM (lower image of Figure 1b) and AFM images (Figure 1c).

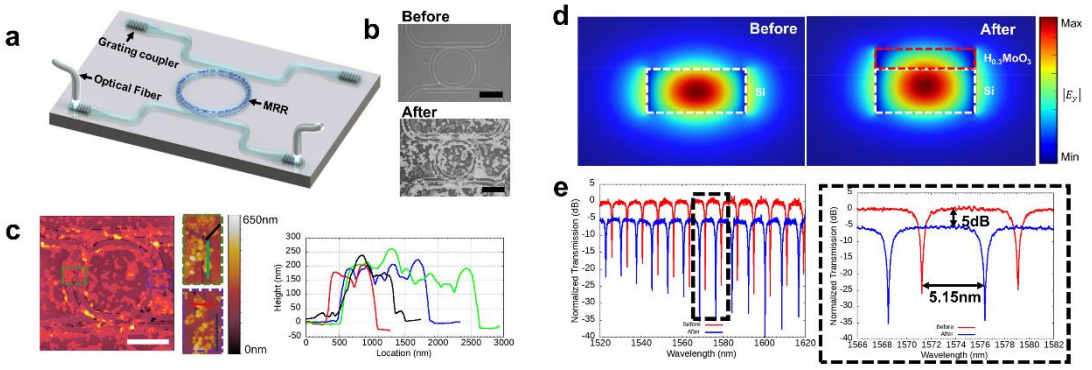

Figure1. a. Schematics of the used device; b. The scanning electronic microscope (SEM) images of the micro-ring resonator before and after $H_{0.3}MoO_3$ deposition. c. Atomic force microscope (AFM) images of the micro-ring resonator after H^+ doped MoO_3 deposition d. Numerical simulation of the optical modes in silicon waveguide before and after H^+ doped MoO_3 deposition. e. The transmission spectrum of the micro-ring resonator before and after H^+ doped MoO_3 deposition.

To explore how the 2D H^+ doped MoO_3 interacts with the silicon optical waveguide, numerical simulation was carried out. The simulation results are shown in Figure 1d. Comparing the optical modes in the waveguide before and after the H^+ doped MoO_3 deposition, the center of the optical mode is lifted, *i.e.* the mode confinement in silicon waveguide is weaker, and the evanescent field of the optical mode penetrates the whole layer of the deposited 2D H^+ doped MoO_3, which indicates the strong interaction between the optical mode in the silicon waveguide and the deposited $H_{0.3}MoO_3$. It also indicates that any change in the deposited 2D H^+ doped MoO_3 layers will affect the optical mode in the silicon waveguide.

The interaction between 2D H^+ doped MoO_3 and optical mode is also reflected on the alteration of the optical performance of the device. Figure 1e shows the measured transmission spectra before and after 2D H^+ doped MoO_3 deposition. As can be seen in the results, the resonant wavelength red shifts about 5.15 nm, and the transmission power drops about 5 dB. The resonant wavelength shift is caused by the fact that the deposited 2D H^+ doped MoO_3 material on micro-ring resonator changed the environment refractive index, which in turn caused the resonant wavelength shift.

3. RESULTS AND DISCUSSIONS

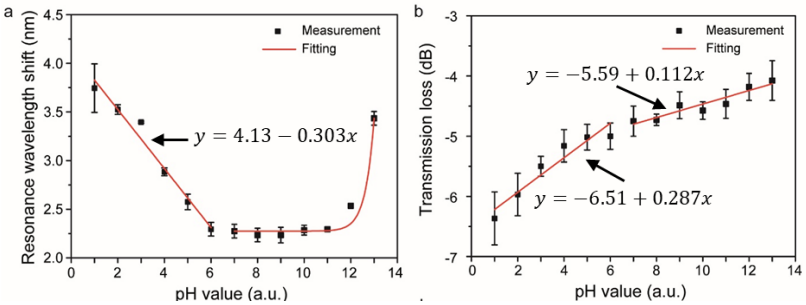

Figure2. (a). MRR resonant wavelengths of the integrated sensors as a function of pH values. (b). MRR transmission power of the integrated sensors as a function of pH values.

The ultra-sensitive ion-responsive sensor is evaluated using pH sensing as a demonstration model. Figure 2 shows the dependence of the transmission spectrum of the micro-ring resonator on the solvent pH value applied. In the measurement, two properties were analyzed, the resonant wavelength and the transmission loss of the micro-ring resonator. Figure 2b shows the transmission spectra of the MRR after 2D H^+ doped MoO_3 deposition for different pH value solvents. As can be seen, the resonant wavelength shifts for different pH values. With increasing pH value from 1 to 6, the resonant wavelength almost linearly shifts to longer wavelengths with the decreasing step of 0.32 ± 0.02 nm per pH. However, for pH values from 7 to 11, there is little change in the resonant wavelength possibly due to insufficient OH^- ions to interact with H^+ doped MoO_3. From pH 11 to 13, the resonant wavelength exponentially shifts to the longer wavelength side. Figure 2b shows the dependence of the relative

transmission loss on the solvent pH value. As can be seen, the transmission loss decreases almost linearly with the increase of the pH value, with the step of 0.2 dB for pH 1 to 6, and 0.15 dB for pH 11 to 13.

4. CONCLUSIONS

An ultra-sensitive silicon photonic based ion sensor was introduced. By integrating with dopant-driven plasmonic nanomaterials onto the silicon photonic platform, this novel ion sensor was enabled with unique ion-responsive capabilities which bare and biomolecule-functionalized silicon photonics were not able to provide. A proof of concept demonstration using a pH sensing model, has shown that the perturbation of ambient ions significantly changes the H+ dopant content and the concurrently injected free electrons in 2D plasmonic molybdenum oxides, leading to a reversible transition between semiconducting and metallic states. The dielectric properties were therefore altered, resulting in the strong influence on the resonant properties of silicon photonics due to the strong coupling of the evanescent field onto the 2D plasmonic layer. Simultaneously, the NIR plasmonic absorption of the 2D layer was affected accordingly, tailoring the light transmission property of the silicon photonic due to the matching between the plasmonic resonance and silicon operation wavelengths. As a result, the sensor could provide dual complementary outputs based on the variation of resonant wavelength shift and transmittance, leading to a wide pH detection range from 1 to 13 with a considerable response linearity. We believe that this work provides a feasible solution to realize on-chip and low-cost ion micro-sensors with high sensitivity, selectivity and repeatability for ionic changes. More importantly, the combination of this 2D plasmonic material with conventional biorecognition elements will potentially widen the applicability of silicon photonic based sensors and will have a notorious impact in the development of more advanced and sophisticated biosensors.

ACKNOWLEDGEMENTS

The authors acknowledge the generous support of the Australian Research Council (CE110001018, DP150101336 and DE160100715). Furthermore, the authors acknowledge the facilities, and the scientific and technical assistance, of the Micro Nano Research Facility (MNRF) and the Australian Microscopy & Microanalysis Research Facility at RMIT University. This work was performed in part at the Melbourne Centre for Nanofabrication (MCN) in the Victorian Node of the Australian National Fabrication Facility (ANFF).

REFERENCES

[1] R. Soref, "The Past, Present, and Future of Silicon Photonics," *IEEE Journal of Selected Topics in Quantum Electronics,* vol. 12, no. 6, pp. 1678-1687, 2006.

[2] A. Rickman, "The commercialization of silicon photonics," *Nature Photonics,* vol. 8, no. 8, pp. 579-582, 2014.

[3] A. H. Atabaki *et al.*, "Integrating photonics with silicon nanoelectronics for the next generation of systems on a chip," *Nature,* vol. 556, no. 7701, pp. 349-354, 2018/04/01 2018.

[4] M. Iqbal *et al.*, "Label-Free Biosensor Arrays Based on Silicon Ring Resonators and High-Speed Optical Scanning Instrumentation," *IEEE Journal of Selected Topics in Quantum Electronics,* vol. 16, no. 3, pp. 654-661, 2010.

[5] S. M. Lo, S. Hu, G. Gaur, Y. Kostoulas, S. M. Weiss, and P. M. Fauchet, "Photonic crystal microring resonator for label-free biosensing," *Optics Express,* vol. 25, no. 6, pp. 7046-7054, 2017/03/20 2017.

[6] A. Parkin, K. E. Dunn, M. G. Scullion, T. F. Krauss, and S. D. Johnson, "The electrophotonic silicon biosensor ´," *Nature Communications,* vol. 7, pp. 1-7, 2016.

[7] S. M. Grist *et al.*, "Silicon photonic micro-disk resonators for label-free biosensing," *Optics Express,* vol. 21, no. 7, pp. 7994-8006, 2013/04/08 2013.

[8] C. S. Huertas, S. Domínguez-Zotes, and L. M. Lechuga, "Analysis of alternative splicing events for cancer diagnosis using a multiplexing nanophotonic biosensor," *Scientific Reports,* Article vol. 7, p. 41368, 01/25/online 2017.

[9] V. Huber *et al.*, "Cancer acidity: An ultimate frontier of tumor immune escape and a novel target of immunomodulation," *Seminars in Cancer Biology,* vol. 43, pp. 74-89, 2017/04/01/ 2017.

[10] I. Kolosenko, S. Avnet, N. Baldini, J. Viklund, and A. De Milito, "Therapeutic implications of tumor interstitial acidification," *Seminars in Cancer Biology,* vol. 43, pp. 119-133, 2017/04/01/ 2017.

[11] G. Fiori *et al.*, "Electronics based on two-dimensional materials," *Nature Nanotechnology,* vol. 9, no. 10, pp. 768-779, 2014.

[12] F. Xia, H. Wang, D. Xiao, M. Dubey, and A. Ramasubramaniam, "Two-dimensional material nanophotonics," *Nature Photonics,* vol. 8, no. 12, pp. 899-907, 2014.

[13] A. K. Geim and I. V. Grigorieva, "Van der Waals heterostructures," *Nature,* Perspective vol. 499, p. 419, 07/24/online 2013.